

IC Models Accounting for Effects of EM Noise

Original

IC Models Accounting for Effects of EM Noise / Stievano, IGOR SIMONE; Canavero, Flavio; Vialardi, E.. - STAMPA. - (2008), pp. 1-5. (International Symposium on Electromagnetic Compatibility (EMC Europe 2008) Hamburg (GE) Sep. 8-12, 2008) [10.1109/EMCEUROPE.2008.4786848].

Availability:

This version is available at: 11583/1957669 since:

Publisher:

IEEE

Published

DOI:10.1109/EMCEUROPE.2008.4786848

Terms of use:

This article is made available under terms and conditions as specified in the corresponding bibliographic description in the repository

Publisher copyright

(Article begins on next page)

IC Models Accounting for Effects of EM Noise

Igor S. Stievano, Flavio G. Canavero and Enrico Vialardi

Politecnico di Torino, Dipartimento di Elettronica,
Torino, Italy, {igor.stievano,flavio.canavero, enrico.vialardi}@polito.it

Abstract— This paper addresses the generation of enhanced models of digital ICs. The proposed models accurately represent the effects of the fluctuations of the device port signals induced by EM disturbances coupling to the system interconnect. The models can be easily estimated from the device port transient responses and can be effectively implemented in any commercial tool as SPICE subcircuits. Model accuracy is assessed by comparing measurements carried out on a test board and simulations. The effects of both continuous wave sinusoidal and pulsed disturbances are discussed.

Keywords: Immunity, Digital ICs, device models, simulation.

I. INTRODUCTION

Nowadays, many commercial electronics equipments that are mounted on vehicles or airplanes and that provide the circuitry needed for the transmission of the information between the different subsystems in the vehicle operate in a noisy EM environment. In these applications, the disturbances possibly generated by the coupling of external fields to system interconnects might affect the proper operation of the system. These equipments must therefore satisfy severe reliability constraints in terms of signal integrity and electromagnetic compatibility and require the assessment of their performances at the early stage of the design phase. Within this framework, the performance assessment is best carried out via numerical simulation where the most critical elements are the models of the digital circuits.

In this paper, we propose a systematic study of the effects of RF noise directly or indirectly coupled to digital systems. This study will lead to the generation of accurate and efficient macromodels of digital devices, accounting not only for their functional behaviour, but also providing insights on their RF immunity. Predictions obtained by means of the proposed IC macromodels and SPICE simulations are compared to actual measurements carried out on a real test board.

II. TEST SETUP

For the sake of simplicity, the study is conducted on a data communication link composed by two digital devices interconnected by a PCB trace. In order to inject the RF noise into the system, the test board shown in Fig. 1 has been designed as suggested by [1]. The board implements the idea of injecting a disturbance through a

long coupled interconnected structure. The two devices, i.e., a driver on the right side in Fig. 1 and a receiver on the left, are connected to terminals 4 and 2 of the coupled structure, respectively. A RF generator is connected to the terminal 3 and a 50 Ω matching resistor to terminal 1. The interconnection, that has a length of 25 cm, is designed to maximize the coupling between the signal communication line and the aggressor trace carrying the RF disturbance. In this study, the two digital ICs in Fig. 1 are simple inverter gates (TI SN74AUC1G04DBVR), optimized for 1.8-V operation. This simplified structure and the two inverters are considered to avoid the complexity of real ICs mounted on an application board and thus allowing to completely understand and model the RF immunity of a digital circuit.

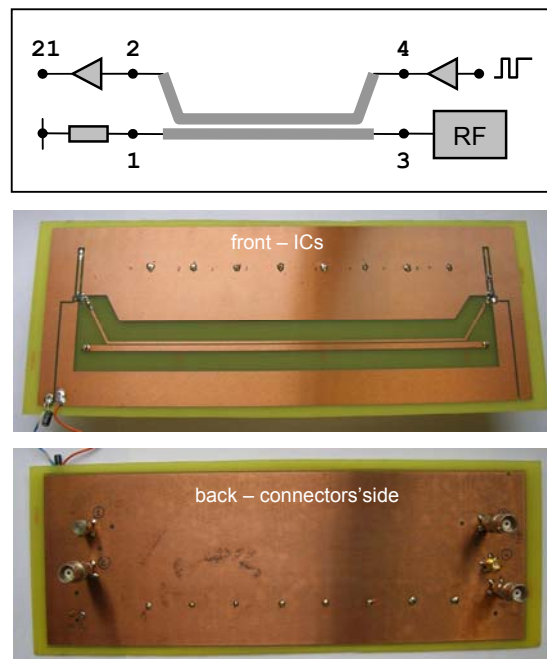


Fig. 1. Ideal setup designed to inject the RF noise into a digital IC (top panel). Test board (bottom panels).

In this work, all the parts composing the complete system in Fig. 1, i.e., the coupled interconnect and the two devices, are modeled by means of suitable modeling methodologies, as suggested in [2]. All the models are

then implemented in SPICE in order to simulate the complete interconnected structure.

In particular, the macromodels for the two digital devices are obtained by means of the state-of-the-art M π log (Macromodeling via Parametric Identification of Logic Gates) methodology [3]. A brief review of the M π log technique is provided in Section III.

The coupled line structure on the board was characterized by means of a two-port network analyzer that has provided a complete set of S parameters up to 2 GHz. These measurements were used to generate a model of the linear interconnect, by means of the IdEM (Identification of Electrical Macromodels) methodology [4]. IdEM is a modeling technique based on the estimation of a reduced order rational approximation reproducing the port behaviour of a complex linear structure from their port responses. The approximation is performed via the powerful and well-known Vector Fitting (VF) algorithm [5], with an a-posteriori correction to assure the passivity of the obtained rational model [6]. Fig. 2 shows a selection of port frequency responses; the comparison of measurements and fitting highlights the accuracy of the obtained model to reproduce the real measurements.

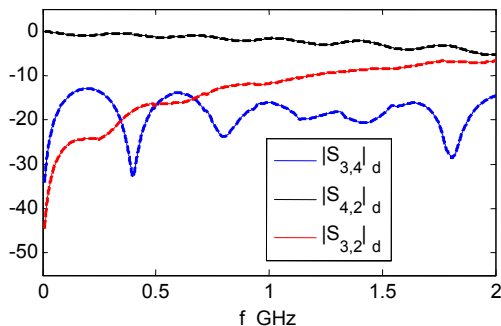


Fig. 2. Selection of S parameters of the test board in Fig 1. Solid lines: measured parameters; dashed lines: model responses.

III. IC MODELS

In this Section, we briefly review the M π log approach [2-3], providing an effective methodology for the construction of accurate and efficient behavioral models of logic devices. This approach amounts to the estimation of parametric relations from suitable device port transient responses. The device stimuli are voltage sources devised to excite every possible dynamic behaviour of the port within a predefined bandwidth, thus allowing the obtained models to account for both the functional and the out-of-band behaviour of devices.

As an example, output buffer constitutive relations are sought as dynamic nonlinear parametric two-piece models of the form

$$i(t) = w_H(t) i_H(v(t), d/dt) + w_L(t) i_L(v(t), d/dt) \quad (1)$$

relating the port voltage v and current i variables, where i_H and i_L are parametric submodels describing the port behaviour in the HIGH and LOW logic states, respectively, and $w_H(t)$ and $w_L(t)$ are weighting coefficients describing state transitions. Parametric nonlinear relations and system identification methods like those involving the identification of mechanical systems, economic trends, etc. allow us to obtain improved nonlinear dynamic models for submodels $i_{H,L}$ in the above representation. Parametric models are usually expressed as sums of basis (e.g., sigmoidal) functions of the involved variables and their parameters are estimated by fitting the model responses to suitable transient responses of the input and output variables related by the model. In this case, the related variables are the voltage and current of the output port in fixed logic state and the model parameters are computed by minimizing a suitable error function between voltage and current waveforms of the model and real device. Specific algorithms are available to solve this problem, depending on the choice of the family of basis functions used to define the parametric models [3].

Parametric models offer rigorous mathematical foundations, identifiability from external observations, good performances for the problem at hand as well as preserving the ability to hide the internal structure of the modeled devices. Finally, parametric models can be readily implemented according to standard industrial simulation tools like SPICE and VHDL-AMS. In addition, such already-mentioned SPICE and VHDL-AMS implementations are completely compatible with the multilingual extension of IBIS (Input/output Buffer Information Specification), which is the most established standard for the behavioral description of IC ports. In fact, ver. 4.1 of IBIS specification [7] is an extension, recently devised to overcome some limitations of the original standard, allowing for more general models not necessarily based on simplified circuit interpretations.

Details on parametric modeling of single-ended CMOS devices, possibly accounting for the device temperature, the power supply voltage, and the power supply current drawn by buffers, can be found in [3], where the parametric approach is applied to the modeling of input and output ports of commercial devices by means of the transient responses of their transistor-level models. The estimation of parametric models from measured transient responses is demonstrated in [8]. Recent advances on the modeling of receiver circuits, including the logic detection mechanism and the effects of power supply voltage fluctuations are reported in [9]. Finally, results on the modeling of differential Low Voltage Differential Signaling (LVDS) devices are described in [10].

The M π log modeling procedure discussed in this Section is applied to build the macromodels for the two ICs mounted on the test board of Fig. 1. For this study,

the models are obtained from the responses of detailed transistor-level descriptions of the devices that are freely available from the official website of the vendor. These macromodels are computed for a power supply voltage of 1 V, which will be hereinafter used for carrying out our study. This supply level, which is close to the lower limit indicated by the manufacturer, was adopted since it is representative of the most critical bias conditions of the device for its noise immunity.

The obtained M π log models are implemented as SPICE subcircuits and then validated by comparing measurements and simulation results of the complete interconnected structure of Fig. 1 in the absence of any RF noise (i.e., the RF source is not connected and is replaced by a matching resistor of 50 Ω). The model results are in excellent agreement with measurements, as already documented in the literature [3,8] (detailed results are not reported here for lack of space).

IV. IMMUNITY ASSESSMENT

In this Section, the test board shown in Fig. 1 is used to perform a systematic set of measurements aimed at the assessment of the immunity of the receiver circuit mounted on the left side of the board. As already outlined in the introduction, a RF generator with 50 Ω internal impedance and a variable frequency and power is used to inject a disturbance into the communication system. In this study, both a disturbance defined by a continuous wave (CW) sinusoidal signal and by a pulsed signal are considered.

CW disturbance. As a first test, the effect of CW sinusoidal disturbances is assessed. The average power of the disturbance, which couples with the functional signals transmitted on the communication line, is increased to verify the receiver immunity thresholds. For this reason, the voltage signal at input terminal 2 of the receiver and the transmitted voltage at terminal 21, i.e., the data processed by the receiver circuit, are monitored to verify possible communication errors. It is worth to remark that the noise immunity of the driver is not considered since, for technological reasons, the internal circuitry of a driver is much more immune to a disturbance injected into its output port. In this experiment, the RF generator produces a 267 MHz sinusoidal waveform and its power is varied between 10 and 23 dBm. The input terminal 41 of the driver circuit is instead connected to a waveform generator producing a square wave signal, i.e. a 010 cyclic bit stream, with a period of 100 ns. A digital scope (Lecroy WavePro 7000A Series) and passive voltage probes (Tektronix P6114B) with a bandwidth of 3 GHz are used to record the voltage signals along the propagation path. Similar results are obtained with different frequencies within the range 100MHz-1GHz.

In order to verify the feasibility of the proposed modeling approach to predict the immunity effects of

devices, the agreement between real measurements and simulations is assessed. The macromodels obtained for both the devices and the coupled line are used together in a SPICE environment to simulate the complete interconnected structure of Fig. 1. It is worth adding that the lumped equivalents of the voltage probes, as provided by the supplier, are included in the simulation setup to reproduce the real measurements.

Figure 3 shows an example of a comparison between measured and predicted responses for the voltage signal at the input (terminal 2) and at the output (terminal 21) ports of the receiver when the power of the RF generator is 10 dBm. The plots are obtained by wrapping in time twenty different periods of the receiver port voltage responses. This comparison highlights that the accuracy of signals predicted by the macromodels are in very good agreement with actual measurements. Besides, the differences between measurements and simulations are mainly due to the model that has been generated from the transistor-level description of devices. Better results could be obtained for models generated from measured data as suggested in [8]. It is also worth to notice that, in this case, the power of the injected disturbance is not sufficient to generate errors in the transmission of the functional signal, even if the input voltage of the receiver has a quite large amount of noise superimposed to the functional part of the signal.

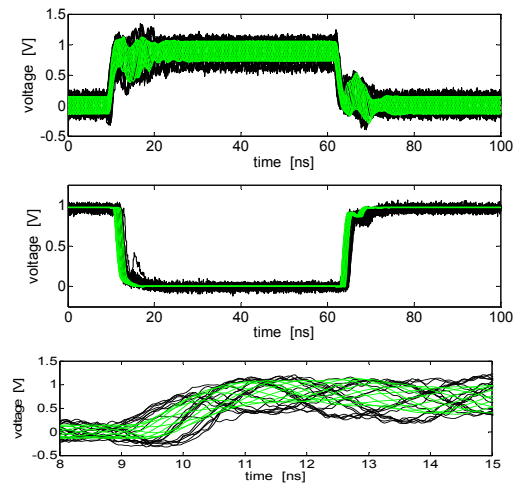


Fig. 3. Voltage signals at input port (top panel) and output port (middle panel) of the receiver for an injected RF noise level of 10 dBm. Zoom of the input port voltage signal (bottom panel). Black lines: measurements; green lines: simulations.

The power of the injected RF signal is then increased to verify potential errors of the received bit at terminal 21. Table I collects the main results of the study and provides in a compact form the information for both the received data 0 (output of the receiver at low state) or 1 (output of the receiver at high state). Each cell of the table collects the information on the possible errors of the received bit. The keywords *yes*, *no* and *possible* are

used, where the latter one is used to provide the information that some glitches are observed in the corresponding H or L states, thus leading to possible error detections at the output of the receiver. An example of this behaviour is the simulation curves reported in the bottom panel of Fig. 4, where results of the RF injection of 16 dBm are shown. In this case, the low state is perturbed just after the switching by some spurious transitions which can generate faults in the data communication link.

Table I. RF Immunity of the Receiver at fixed High and Low States

RF power level (dBm)	errors @ receiver output - V21 (measurements / simulations)	
	HIGH state	LOW state
10	no / no	no / no
13	no / no	possible / possible
16	no / no	yes / possible
20	possible / possible	yes / yes
23	yes / yes	yes / yes

Moreover, the 16 dBm test case shows an asymmetric behaviour of the device immunity for the two logic states: the H state is more robust than the L one. In fact (see Table I), a RF level of 23 dBm must be injected in the system for inducing regular faults in the high state, whereas a noise power of 13 dBm might lead to errors in the low state.

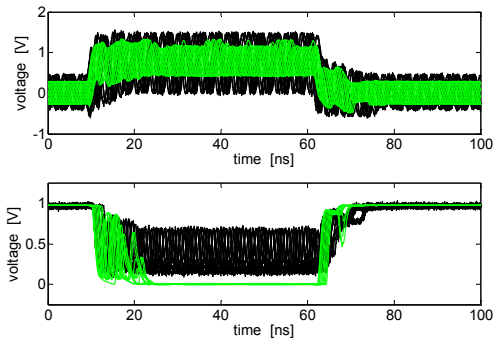


Fig. 4. Voltage signals at input port (top panel) and output port (bottom panel) of the receiver for an injected RF noise level of 16 dBm. Black lines: measurements; green lines: simulations.

Even in such a critical situation of asymmetry, the $M\pi$ log approach proves its capabilities to predict the device behavior. Only in the L logic state of the test with a RF power of 16 dBm, a discrepancy between the model and the measurements can be observed in the bottom panel of Fig. 4. This effect can be more clearly explained by observing the top panel of the same figure, that shows the voltage at the input port of the receiver (terminal 2): a difference on the amplitude of the oscillations between measurement and simulation, especially for the H input state, lead to a possibly different processed signals at the output of the receiver.

This observation confirms the interest in generating the $M\pi$ log models from real measurements carried out on a real board.

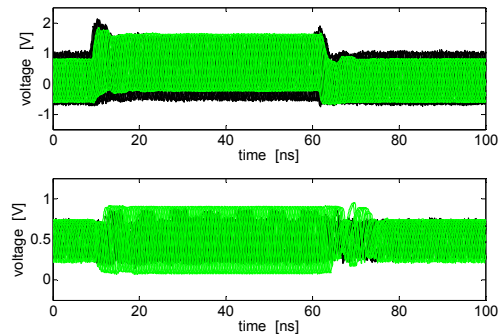


Fig. 5. Voltage signals at input port (top panel) and output port (bottom panel) of the receiver for an injected RF noise level of 23 dBm. Black lines: measurements; green lines: simulations.

Finally, when the injected power reaches 23 dBm (Fig. 5), the receiver is no longer able to reproduce at its output port the functional signal, both for the L and the H state, but such signal is so distorted that it appears to be almost a replica of the injected noise disturbance. Also in this case, the $M\pi$ log models (even if extracted from a transistor-level description of the example devices) offer good quality predictions of the out-of-band and out-range behaviour of the devices.

Pulsed disturbance. To complement the CW case, a second set of experiments is carried out by considering a pulsed noisy signal. The disturbance is obtained by modulating a sinusoidal carrier with a square wave signal with variable period and duty cycle. The MA-COM 96341switch is used to combine a 900 MHz sinusoidal signal with a 9MHz square wave signal. The Agilent ESG E4433B and 22220A programmable sources are used to generate the carrier and the modulating signals, respectively. The amplitude of the carrier and the duty cycle of the modulating signal are then tuned to modify the peak power and the average power of the pulsed disturbance.

As already done for the CW case, a large number of comparisons between measurements and simulations is carried out. As an example, Fig. 6 shows the measured and the predicted responses of the voltage signal at the input (terminal 2) port of the receiver when the driver mounted on the right side of the board of Fig. 1 keep the signal line in the fixed high state. In this comparison, the power of the sinusoidal carrier is 7 dBm and the duty cycle of the modulating signal is $D=20\%$ or $D=50\%$. Also for this case, the good agreement between measurements and predictions confirms the accuracy of the proposed models.

It is also worth noting that for the class of disturbances considered in this study and defined by a

RF carrier within the range 100-900MHz modulated by a some MHz square wave signal, the same results obtained for the CW case are confirmed. As an example, Fig. 7 compares the measurements of the input port of the receiver (terminal 2) obtained when the disturbance is either a CW or a pulsed signal. In this test, the CW signal is again a 900MHz sinusoidal signals with 11dB of power and the pulsed disturbance is defined by the CW signal with variable power modulated by a 9MHz square wave signal.

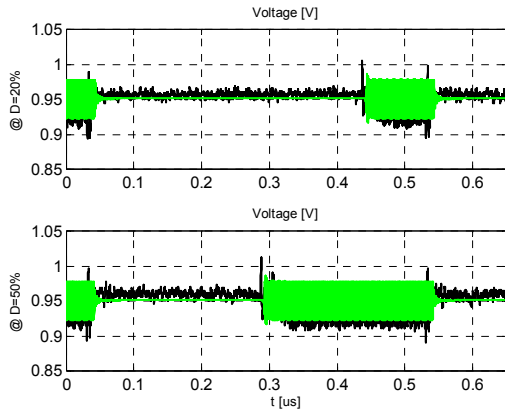


Fig. 6. Voltage signals at input port of the receiver for different values of the average injected power, i.e., for different duty cycle of the pulsed disturbance. Black lines: measurements; green lines: simulations.

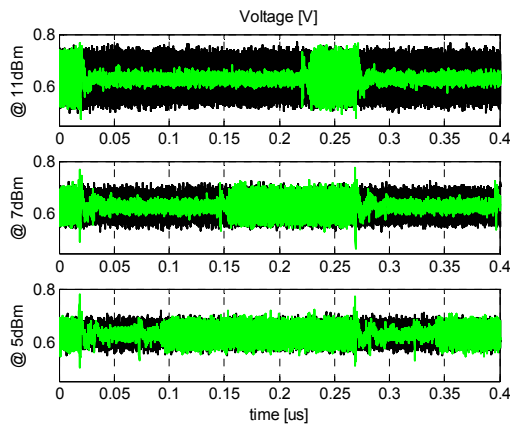


Fig. 7. Measured voltage signals at input port of the receiver for different values of the injected RF noise level. Black lines: CW case; green lines: pulsed case.

CONCLUSIONS

This paper describes a preliminary application of the systematic M π log methodology for the modeling of the noise immunity of inverter gates representing the input ports of digital ICs. Obtained results highlight the capability of the proposed approach to model both the functional and the out-of-band behaviour of such devices. Next steps towards the generation of a complete IC macromodel will have to focus on the injection of RF noise into the power supply net of the device and on the modeling of these effects.

REFERENCES

- [1] J. S. Bazzoli, B. Démoulin, M. Cauterman, P. Hoffmann, Susceptibility of integrated circuits connected to wiring systems, Proc. of IEEE Symposium on Embedded EMC (2EMC), Rouen, France, Sep. 2005.
- [2] F. G. Canavero, S. Grivet-Talocia, I. A. Maio, I.S.Stievano, Linear and nonlinear macromodels for system-level signal integrity and EMC assessment, IEICE Trans. on Communications - Special Issue on EMC, vol. E88-B, no. 8, pp. 1121-1126, Aug. 2005.
- [3] I. S. Stievano, I. A. Maio, F. G. Canavero, M π log, macromodeling via parametric identification of logic gates, IEEE Transactions on Advanced Packaging, vol. 27, n. 2, pp. 15-23, Feb. 2004.
- [4] Modeling tools of the EMC group available at <http://www.emc.polito.it>.
- [5] B. Gustavsen, A. Semlyen, Rational approximation of frequency responses by vector fitting, IEEE Transactions on Power Delivery, vol. 14, pp. 1052-1061, July 1999.
- [6] S. Grivet-Talocia, Passivity enforcement via perturbation of Hamiltonian matrices, IEEE Transactions on CAS-I, vol. 51, n. 9, pp. 1755-1769, Sept. 2004.
- [7] I/O Buffer Information Specification (IBIS) Ver. 4.1, on the web at <http://www.eigroup.org/ibis/ibis.htm>.
- [8] I. S. Stievano, I. A. Maio, F. G. Canavero, Behavioral models of I/O ports from measured transient waveforms, IEEE Transactions on Instrumentation and Measurement, vol.51, no. 6, pp. 1266-1270, Dec. 2002.
- [9] I. S. Stievano, F. G. Canavero, I. A. Maio, Behavioral macromodels of digital IC receivers for analog-mixed signal simulations, Electronic Letters, 2005.
- [10] I. S. Stievano, I. A. Maio, F. G. Canavero, C. Siviero, Parametric macromodels of differential drivers and receivers, IEEE Transactions on Advanced Packaging, vol. 28, no. 2, pp. 189-196, May 2005.